

TOKES studies of the thermal quench heat load reduction in mitigated ITER disruptions



S. Pestchanyi^{a,*}, M. Lehnen^b, R.A. Pitts^b, G. Saibene^c

^aKIT, Hermann-von-Helmholtz-Platz 1, Eggenstein-Leopoldshafen, Germany

^bITER Organization, Route de Vinon-sur-Verdon, CS 90 046, 13067 St. Paul Lez Durance Cedex, France

^cFusion for Energy, 08019 Barcelona, Spain

ARTICLE INFO

Article history:

Received 13 July 2016

Accepted 7 December 2016

Available online 26 December 2016

ABSTRACT

Disruption mitigation by massive gas injection (MGI) of Ne gas has been simulated using the 3D TOKES code that includes the injectors of the Disruption Mitigation System (DMS) as it will be implemented in ITER. The simulations have been done using a quasi-3D approach, which gives an upper limit for the radiation heat load (notwithstanding possible asymmetries in radial heat flux associated with MHD). The heating of the first wall from the radiation flash has been assessed with respect to injection quantity, the number of injectors, and their location for an H-mode ITER discharge with 280 MJ of thermal energy. Simulations for the maximum quantity of Ne (8 kPa m^3) have shown that wall melting can be avoided by using solely the three injectors in the upper ports, whereas shallow melting occurred when the midplane injector had been added. With all four injectors, melting had been avoided for a smaller neon quantity of 250 Pa m^3 that provides still a sufficient radiation level for thermal load mitigation.

© 2017 Elsevier Ltd.

This is an open access article under the CC BY-NC-ND license.
(<http://creativecommons.org/licenses/by-nc-nd/4.0/>)

1. Introduction

The ITER plasma control system is designed to allow reliable and stable operation throughout all discharge phases. It will react to any deviation from the predicted behavior which includes application of active disruption avoidance schemes. Despite these efforts, disruptions caused by plasma instabilities, loss of control events or plant failures cannot be excluded. Should a disruption remain unmitigated, melting and vaporization of the ITER metallic plasma-facing components (PFC) cannot be excluded [1]. A disruption mitigation system (DMS) is being designed for ITER to mitigate the thermal loads deposited during unavoidable disruptions.

The ITER DMS is being designed based on a comprehensive experimental database collected from existing tokamaks. The mitigation strategy relies on the injection of high Z noble gas (NG), namely neon or argon, possibly combined with deuterium for prevention of runaway electrons generation. The injection aims to dissipate the plasma stored energy through an increase in radiation, thereby reducing direct thermal loads to the first wall and divertor PFCs. The system consists of hybrid injectors that are able to act as shattered pellet injectors (SPI) or can be used for massive gas

injection (MGI). These injectors are situated in three of the upper port plugs and in one equatorial port, see Fig. 1.

Disruption mitigation by MGI has been simulated previously for ITER [2] using the TOKES code [3] which has been developed over the past decade at FZK-KIT for integrated 2D simulations of transient events in tokamaks. The simulations include interaction of the plasma with the injected high Z impurities, with the divertor and with the first wall armor in diverted magnetic configurations. Each excitation level of each ion species in plasma treated in TOKES as separate fluid. Dynamics of the level populations is calculated and radiation intensity is calculated according to this dynamics. Comprehensive description of the code has been performed in [3]. The code has been benchmarked against MGI experiments in JET and in DIII-D [4–7]. Recently the TOKES code has been updated to account for 3D effects in radiation heat loads during MGI. MGI in the DIII-D tokamak has also been simulated using the NIMROD code with emphasis given to estimation of toroidal peaking factor of the radiation heat load, see [8–10] and the references there. One should also note first attempt of MGI simulations for JET using JOREK code reported in [11].

The simulations reported here include the ITER first wall geometry and the set-up of the ITER DMS and model the flow from the injector into the vacuum vessel, see Fig. 1. Heat load mitigation has been optimized in the simulations to avoid melting from the radiation flash whilst keeping a radiation level high enough to

* Corresponding author.

E-mail address: serguei.pestchanyi@kit.edu (S. Pestchanyi).

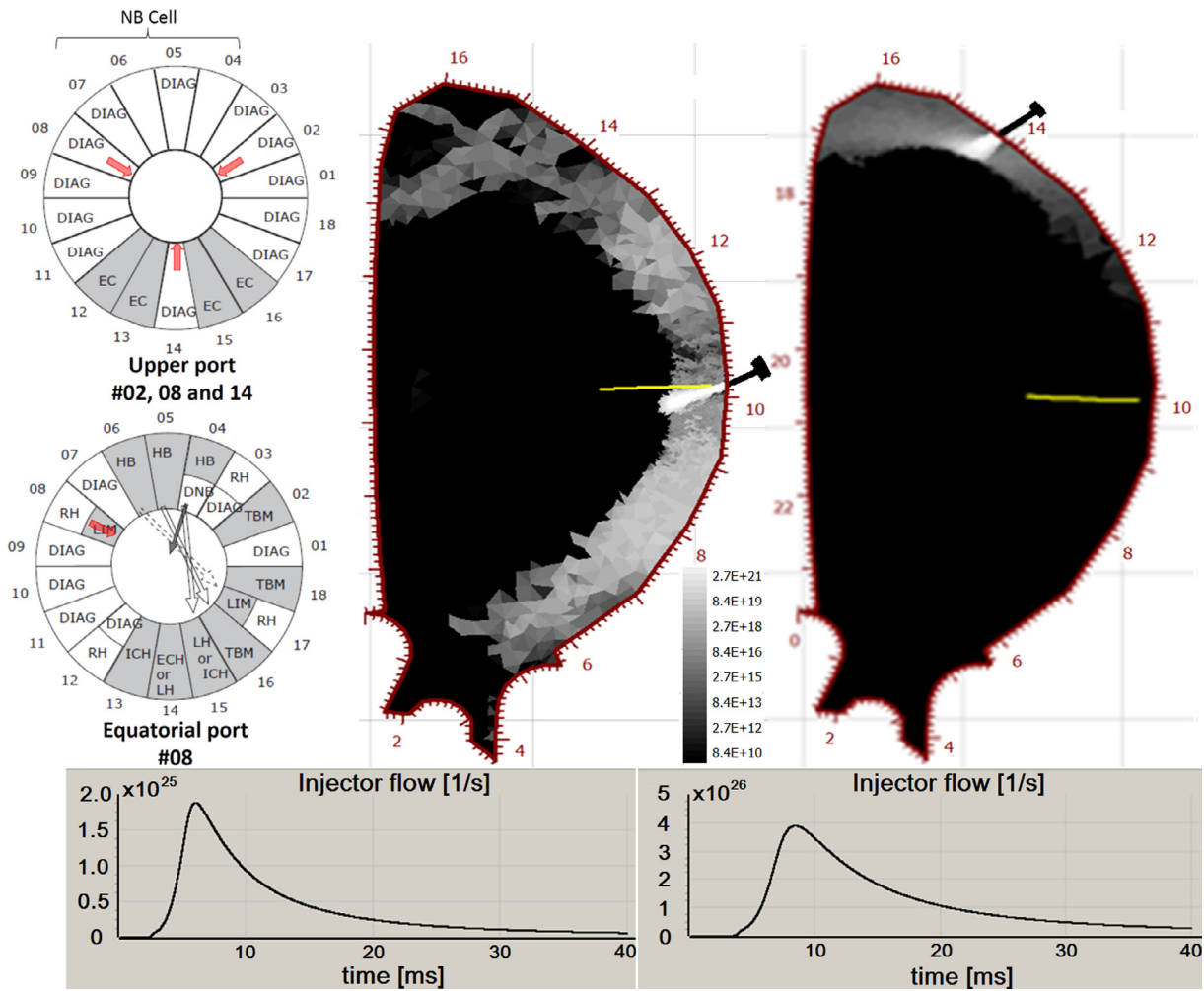


Fig. 1. Arrangement of the injectors of the ITER disruption mitigation system. The positions of the three upper injectors and the midplane injector are shown in the left panel. Examples of Ne flow from the midplane injector and from the upper injector are shown in the middle and right panels. The logarithmic gray scale gives the Ne density. Time dependences for the gas flux from the midplane injector ($P_{0/32}$ particles in the injector plenum) is shown in lower left panel and corresponding flux from the upper injector (P_0) – in lower right panel.

ensure sufficient mitigation of heat loads through conduction. The injection quantity, the number of injectors, and their location have been varied.

2. TOKES technique to account for 3D effects of wall radiation during MGI

2.1. Sketch of 2D TOKES simulation principles

The 2D TOKES code uses fluid plasma dynamics for plasma propagation along magnetic field as well as for diffusion and thermoconductivities across the magnetic field in tokamak magnetic configurations with diverted magnetic field (Braginskii [12] equations for multi-species plasma with ionization-, recombination-, excitation- dynamics and with photonic radiation cooling). Turbulent energy and particles transport during the disruption is simulated by enhancing the cross-field transport coefficients. Noble gas propagation in the injector and its guiding tube is modeled in 1D approximation. Due to the 2D nature of the TOKES code, the injector is simulated as a toroidally symmetric slit, injecting NG uniformly along the toroidal direction. Inside the ITER vacuum vessel (VV) the gas stream is assumed to propagate in a prescribed cone with the conical angle corresponding to the Mach number of the gas stream. The simulation of MGI in the 2D TOKES code starts

from NG propagation in the injector and in the VV. Then, after reaching the separatrix, the NG is ionized in the pedestal, which is cooled down by NG ionization and by photonic radiation from the NG plasma. The edge cooling process is fast compared to stationary transport times, of the order of milliseconds, so that the radial profile of the plasma temperature further inside the plasma remains unaffected and a sharp cooling front builds up that propagates towards the plasma core. In TOKES simulations it is assumed that the thermal quench (TQ) starts when this cooling front reaches the $q=2$ magnetic surface. At that time, the cross-field transport coefficients are increased and the plasma thermal energy is lost to the core outskirts where the radiation from the NG spreads this energy over the surrounding first wall PFCs. Naturally, the radiation heat load in the simulations is toroidally symmetric, distributing the heat uniformly over the entire toroidal circumference of the wall.

2.2. TOKES code modifications to account for 3D effect of point-like injection

In ITER the NG will propagate through the injector tubes of 28 mm diameter with lengths of 6.5 m for the upper injectors and of 4.5 m for the midplane injector. The gas is expected not to cross the separatrix uniformly in toroidal direction, but rather through

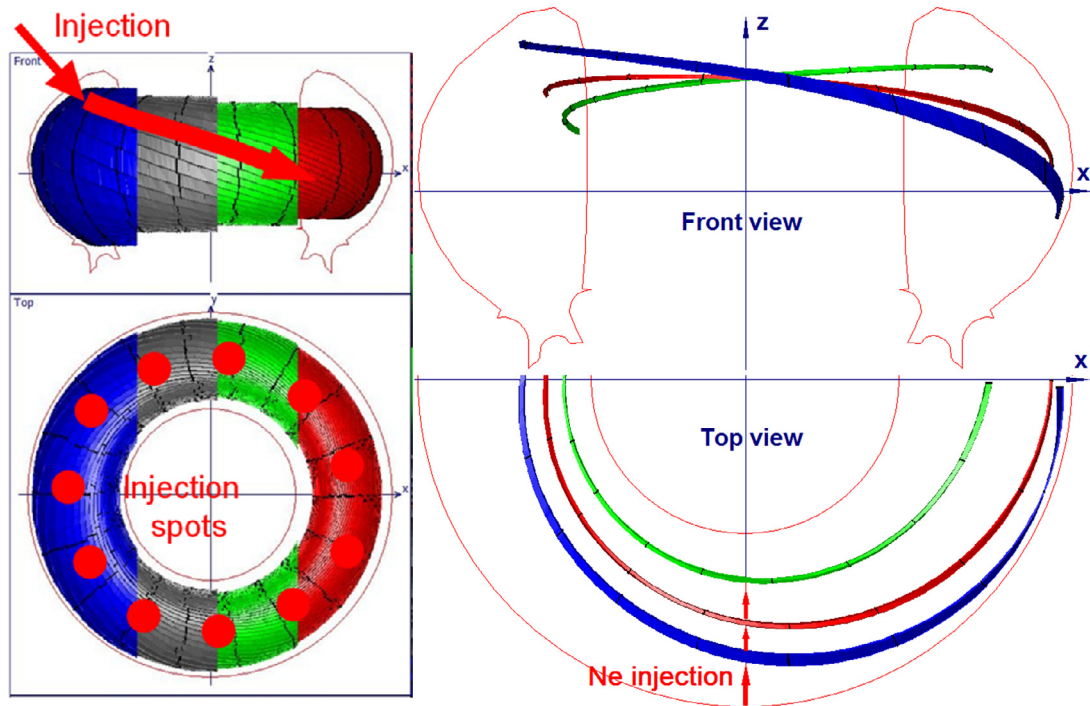


Fig. 2. TOKES 3D magnetic flux coordinates calculation grid is shown in left panel. Various colors indicate sequential layers of cells, each of which are the segments of one continuous magnetic tube, fully covering one magnetic layer. For simulation of plasma dynamics from one ITER injector the torus is 'tiled' with N_{tor} identical blocks, consisting of the radiator, the reservoir and the injector each. N_{tor} injectors are almost identical to one 2D injector of the 2D TOKES. Right panel illustrates Ne gas injection from the midplane injector in y -direction. Shown are parts of the radiators, consequently filled by the injected gas. Ne plasma propagates from the injection point along the radiators in both directions. Shown are three radiators at some radial distance for visibility; in reality the neighboring radiators are touched each other at the injection point. Plot of entire radiator from one layer is shown in Fig. 3. (For interpretation of the references to color in this figure legend, the reader is referred to the web version of this article.)

a spot of 0.5–1 m characteristic size toroidally and poloidally in the vicinity of each injector. The spot size is estimated from the distance $D \sim 0.5 \div 1$ m between the injector and the hot plasma boundary at different stages of the core cooling, accounting the Mach number $M=3 \div 1$ for the gas flowing out of the injector. The TOKES code has been upgraded to take this asymmetry into account. This upgraded version of TOKES is not a full scale 3D model for plasma dynamics during MGI, because it does not take into account plasma transport (diffusion and thermoconductivities) across magnetic field lines inside the magnetic layers of the tokamak. Cross-field transport during TQ runs in two mutually orthogonal directions: inside the magnetic layer and perpendicular to the layers – in radial direction (both perpendicular to the magnetic field). Cross-field transport inside the layers is not taken into account, as mentioned above; however, the disruptive radial cross-field transport is taken into account.

For simulations of the toroidal asymmetry in radiation the TOKES calculation grid (which initially uses 2D nonlinear orthogonal magnetic flux coordinates) has been divided in toroidal direction by N_{tor} equidistant poloidal planes, thus defining a 3D calculation grid. 3D cells of this grid are magnetic flux tubes, running along the magnetic field lines, winding over the core and divided in toroidal direction in N_{tor} segments as shown in Fig. 2. The injection takes place in one of these segments. The magnetic layer is the layer between two neighboring magnetic surfaces, limiting the cells in radial direction. In the TOKES simulations reported here, each layer is fully covered with one closed magnetic tube, winding 60–80 times till it closes in itself.

Dynamics of NG plasma inside the core, simulated by TOKES, is assumed to proceed as follows. First of all, at pre-TQ stage, the NG stream from the injector penetrates into the first magnetic layer (blue layer in Fig. 2). First portions of NG are fully ionized, but

continuous feeding of this layer by NG at the same position forms cold NG plasma spot, which expands along the magnetic field, being heated from hot DT plasma mainly by electron thermoconductivity along the magnetic field and cooled by NG line radiation. After sufficient cooling of the plasma at the injection point, part of the continuously injected NG can cross the first blue layer without ionization and penetrates further into the second magnetic layer (gray one in Fig. 2), causing the same cold NG plasma cloud formation, its expansion along the magnetic field and irradiation of the plasma energy from this layer. This process results in sequential cooling down of several magnetic layers and persists till the start of TQ. One should note that the neutral NG propagation is influenced by resonant charge exchange process; the results of gas cloud dynamics are illustrated in Fig. 1.

TOKES scenario of MGI assumed that TQ starts after cooling down of predefined magnetic surface (with $q=2$). TQ simulated by artificial increase of cross field thermoconductivities (due to start of turbulent plasma energy transport). Increased radial electron thermoconductivity transports plasma thermal energy from core bulk to the core edge contaminated with NG, where the energy irradiated onto surrounding walls. Injection of NG, its ionization and the NG plasma expansion along the magnetic field lines proceeds as usual during TQ, but the turbulent energy transport is much faster, so whole core is cooled down due to radiation from the contaminated external core layers.

In TOKES simulations NG plasma expands along the magnetic field; diffusion of the plasma to the neighboring part of the magnetic tube is neglected. That means the radiation source in each magnetic layer is spanned along the magnetic tube, in which NG injected. During whole simulation time longitudinal span of expanding NG plasma is assumed to be less than one poloidal turn (which equals to q toroidal turns; q is the safety factor and

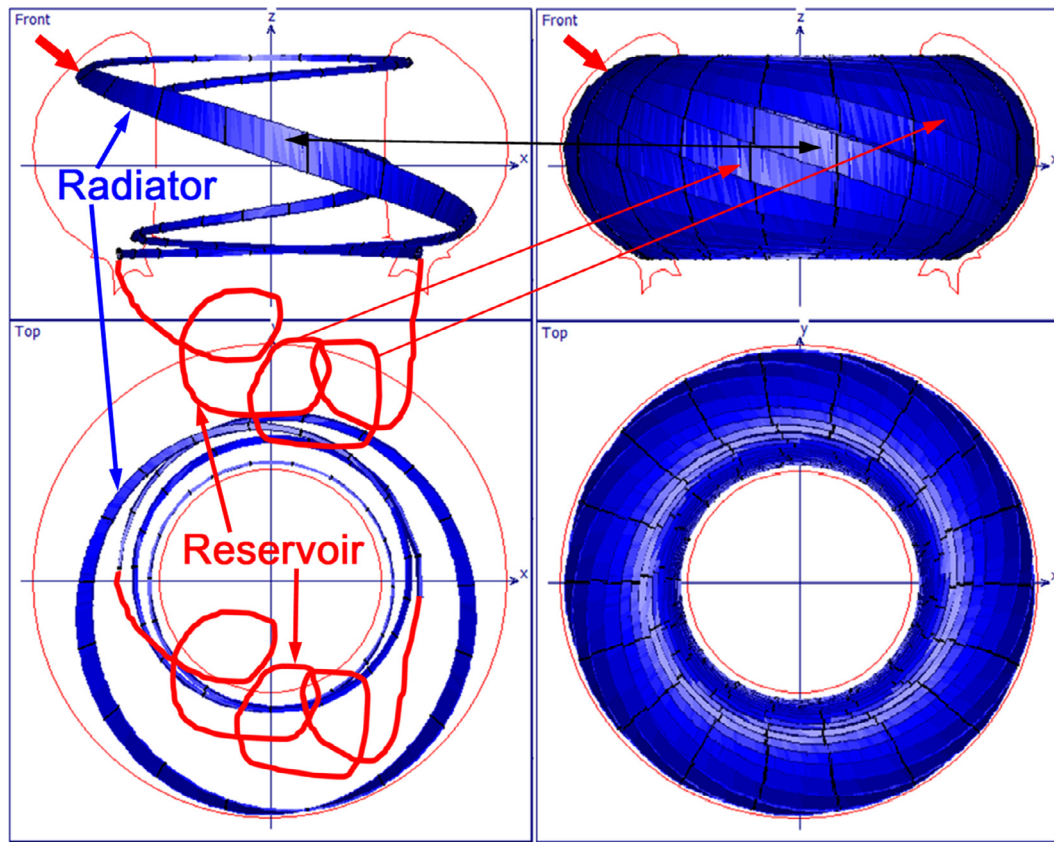


Fig. 3. Contaminated plasma dynamics is assumed along one poloidal turn (the radiator) of the magnetic tube in which the NG is injected (bold red arrow in upper left corner). The radiator is shown from above (left lower panel) and from front (left upper panel) with blue color. The rest of the magnetic tube, covering the entire magnetic surface (right panel) is called in TOKES simulations the ‘reservoir’. The reservoir can be moved to a virtual position, schematically shown by a red tube. Real positions of the reservoir are shown by red arrows. (For interpretation of the references to color in this figure legend, the reader is referred to the web version of this article.)

$2 \leq q < \infty$ close to the separatrix) as shown by blue color in Fig. 3. This one poloidal turn of the tube is called ‘radiator’. The rest of the magnetic tube with DT plasma without NG, called ‘reservoir’, is cooled down due to the electron thermoconductivity along the magnetic field. During TQ the cross field turbulent plasma energy transport heats the NG plasma directly in the contaminated part of the tube, but main radial heat flux heats DT plasma inside the reservoir, which is much larger than the contaminated turn. Then, this heat transported to the radiation cloud by electron thermoconductivity along the magnetic field and radiated onto the first wall also.

Simulation of the above described scenario has been done using special trick, which allows boiling down of 3D problem to 2D simulation of the plasma dynamics, combined with 3D radiation deposition onto the first wall.

Since we assume absence of plasma cross-field transport inside the magnetic layers, the NG plasma will be transported along each magnetic tube independently, without mixing with the neighboring reservoir, covering the layer. Radiation from the radiator heats the wall, so its position relative to the wall is important, but the reservoir may be removed from the layer to some ‘virtual’ position as shown in Fig. 3, because its only role in the process is to transport energy to the radiator. Simulations of the wall heating with the reservoir in the layer and with the reservoir in the virtual position are identical. Bearing this in mind one can define a ‘block’, which consists of a radiator, connected with its reservoir in virtual position and of the injector. Then, one can tile toroidally all the circumference of each layer with N_{tor} blocks side by side. The blocks will be joined with radiators side by side covering whole layer, with the reservoirs in virtual positions and with injectors,

approximating the toroidal slit injector of the 2D TOKES as shown in Fig. 2. The plasma dynamics in each of the blocks proceeds independently one from another and is identical, so the plasma dynamics can be simulated with 2D TOKES code with attached N_{tor} reservoirs and with 2D NG injection increased N_{tor} times.

This algorithm has been used for simulation of the first wall radiation heat load during MGI in ITER with the 2D TOKES code and with modified 3D radiation simulation subroutine, which calculates the heat load from one radiator of each layer only. Positions of these radiators are illustrated in the right panel of Fig. 2. The technique explained above allows taking into account the 3D nature of the radiation heat loads. It should be noted that these heat loads might be overestimated due to the omission of the cross-field transport. Thus, the results reported here give an upper limit of the heat loads (assuming symmetry in the radial cross-field transport) whereas the 2D simulations performed previously give a lower limit due to the uniform impurity distribution in toroidal direction.

Simulation of MGI from N_{inj} injectors, symmetrically distributed over toroidal circumference is also possible. The only difference in this case is the reservoir should be decreased correspondingly.

3. Simulation results

3.1. 2D – 3D simulation results comparison

The results from the two TOKES versions, 2D and 3D, have been compared for an injection of 2 kPa m^3 of Ne gas from each of the three upper injectors into an H-mode ITER plasma with 280 MJ of thermal energy. In the 2D simulation the total Ne gas amount of

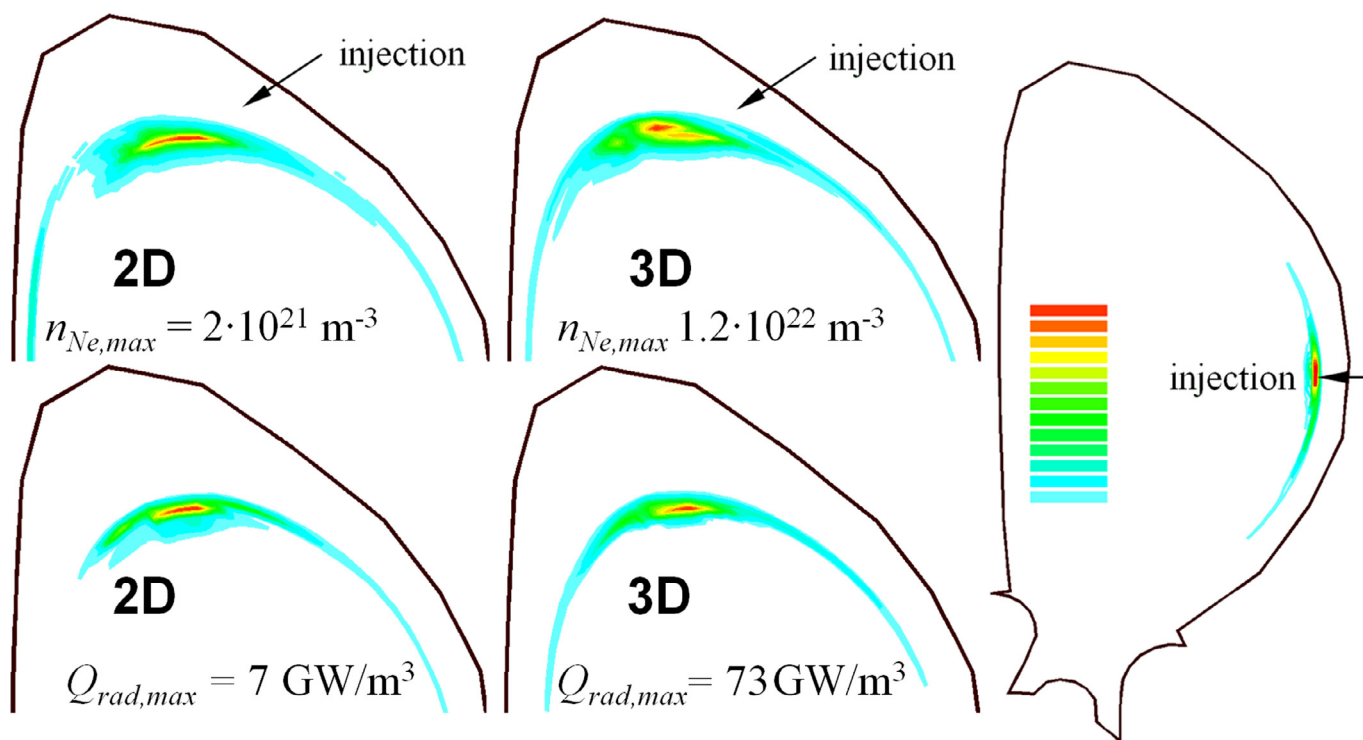


Fig. 4. Results of 2D (two left panels) and 3D (two middle panels) TOKES simulations of the same MGI. Shown are contours for Ne plasma density (two upper panels) and for the radiation intensity (two lower panels) at the upper part of the poloidal plane at 7 ms. On the right panel the radiation intensity from the midplane injector at 5 ms is shown for comparison. Color scale for all the plots is shown; maximum value corresponds to red and minimum to blue color. Maximum Ne plasma density is $1.2 \times 10^{22} \text{ m}^{-3}$ for 3D and $2 \times 10^{21} \text{ m}^{-3}$ for 2D. The corresponding maxima in radiation intensity are 73 GW/m^3 and 7 GW/m^3 . The maximum in radiation intensity for the midplane injector is 110 GW/m^3 . Injector position is indicated by arrow. (For interpretation of the references to color in this figure legend, the reader is referred to the web version of this article.)

6 kPa m^3 has been injected through a toroidally symmetric slit. The simulations show that the contaminated plasma cloud consists of more than 90% of Ne ions and less than on 10% of D-T mixture at the position of maximum density. The Ne plasma density of the 2D simulation and the corresponding projection of the Ne density onto the poloidal plane for the 3D simulation are shown in Fig. 4 at 7 ms, which corresponds roughly to the maximum in radiated power. Note that all times in this paper are given relative to the opening time of the injector valve. The spatial distributions of the neon ions are qualitatively similar for both cases, as seen in Fig. 4. However, the peak Ne density is 6 times larger in the 3D version compared to 2D: $1.2 \times 10^{22} \text{ m}^{-3}$ and $2 \times 10^{21} \text{ m}^{-3}$ correspondingly. The photonic radiation source intensities are given for the same time in the lower panel of Fig. 4. The intensity maxima approximately correlate with the peaks in Ne plasma density, but the maximum value in the 3D simulation is more than 10 times larger than for 2D: 73 GW/m^3 and 7 GW/m^3 , correspondingly. These differences are quite expectable, because in 3D the injected Ne plasma concentrated toroidally close to injectors and in 2D simulation it is evenly distributed along the toroidal angle. In both cases the Ne plasma expands along the magnetic field, but the expansion dynamics are not identical. The plasma energy in each magnetic layer is transported along the magnetic field lines to the location of high Ne ion density where it is radiated and deposited to the surrounding walls. The energy transport is mainly due to electron thermoconductivity, but in the 2D case the transport is over half poloidal turn from both sides of the Ne cloud whereas in the 3D case the transport is over a distance a factor $(N_{\text{tor}}/N_{\text{inj}} - 1) \gg 1$ larger.

Note, that the Ne plasma of noticeable density spans over less than 1/3 of poloidal circumference at 7 ms, see upper panel in Fig. 4. This confirms the assumption, stated in Section 2.2. The

same is valid for the radiation intensity, lower panel in Fig. 4. The radiation intensity spans over less than one poloidal turn up to ~ 20 ms, when almost all the plasma energy is irradiated.

The cross-field transport coefficients during the TQ have been adjusted to ensure a characteristic rise time for the radiated power P_{rad} of 1–2 ms, see Fig. 5. The 3D simulations show a slow decay $P_{\text{rad}}(t)$, which can be explained by the equipartition time between electrons and ions. The thermal energy of the ions is dissipated through the heat transfer to the electrons, further transport by electron thermoconductivity to the radiator and then irradiation from Ne plasma cloud. $P_{\text{rad}}(t)$ decreases within 5–10 ms as seen in the left panel of Fig. 5. The resulting wall heat loads and the corresponding wall temperatures are shown in Figs. 5 and 6. The maximum wall temperature is lower in the 2D simulation compared to 3D due to the more uniform spread of the radiation source. The corresponding maximum wall heat flux is by a factor 2–3 lower. The duration of heat flux deposition on the first wall is longer in the 3D case, which can be expected because of the longer distances over which the plasma thermal energy is transported to the Ne plasma cloud. The poloidal position of the heat flux maxima is similar in both cases, 2D and 3D. But in 3D case the heat flux concentrated in toroidal direction close to the three injectors, whereas it is constant in toroidal direction in the 2D case. The toroidal peaking factor (TPF) of the heat flux on the wall has been calculated in the 3D case to be in the range of 2–3 at the poloidal position where the heat flux maxima from the upper injectors are situated (see Fig. 7). For the poloidal position where the maximum appears for the midplane injector, the TPF is about 10. It is important to note that the heat flux peaks at different times for the upper injectors and for the mid-plane injector. The time difference is about 2 ms for this specific simulation. The poloidal peaking factors (PPFs) are also of the order of 10 for the sections, running through

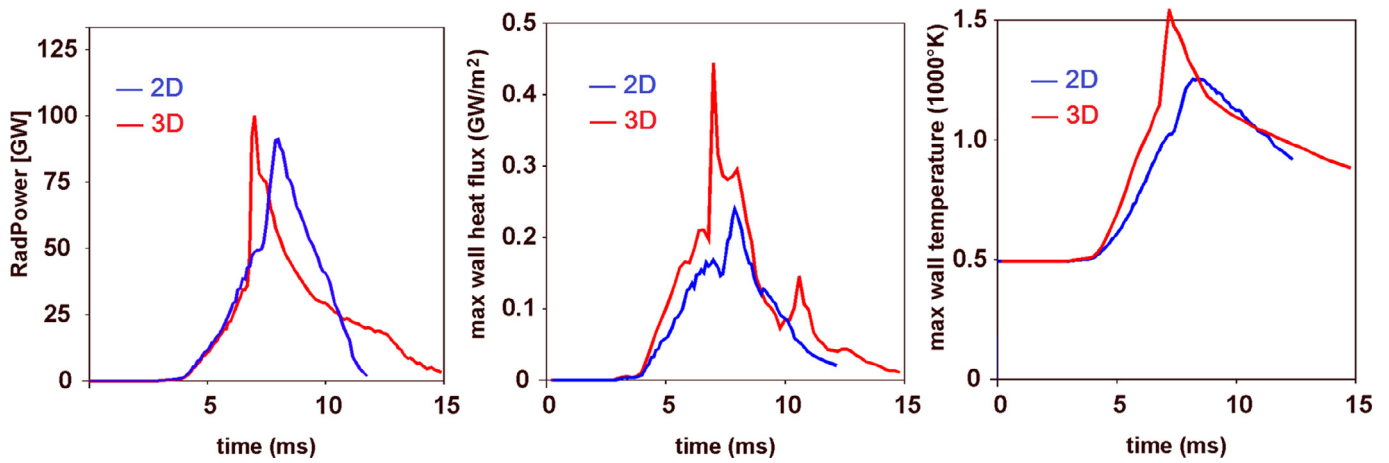


Fig. 5. Comparison of the temporal evolution of the total radiated power from the plasma core (left panel), of the peak wall heat flux (middle panel) and of the peak wall temperature (right panel). The results of 3D simulation are shown with red color and for 2D with blue. The maximum wall temperature in the 2D simulation is smaller than in 3D due to the uniform spread of the radiation source along the toroidal angle. (For interpretation of the references to color in this figure legend, the reader is referred to the web version of this article.)

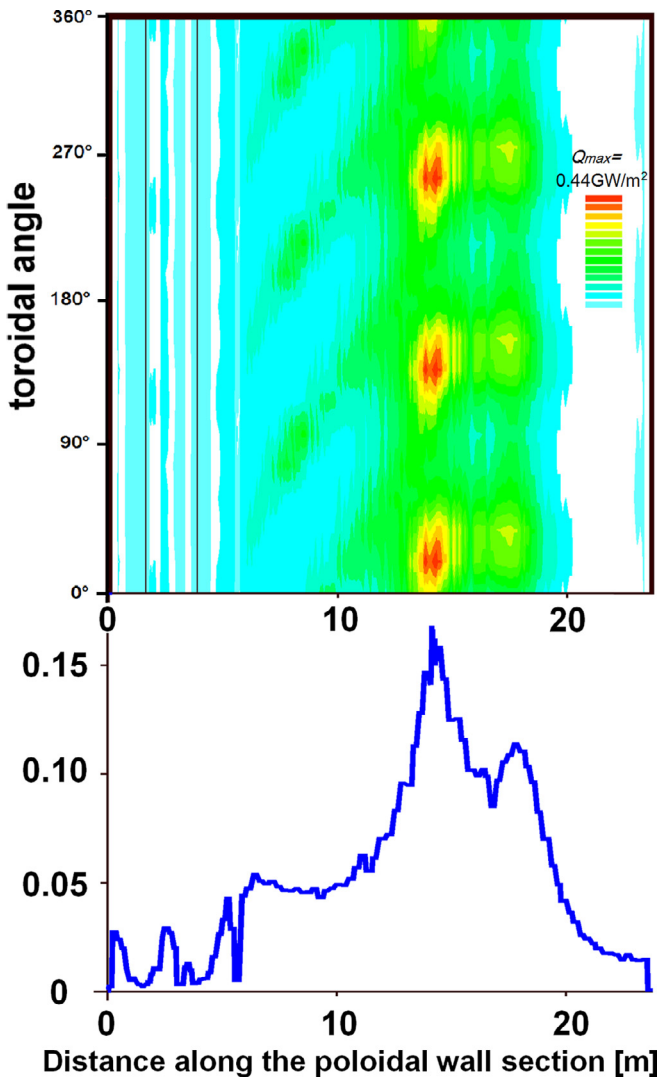


Fig. 6. Wall heat flux distribution over the ITER first wall at 7 ms simulated with the 3D TOKES code (upper panel) and with 2D TOKES (lower panel). The maximum in the color scale (red) corresponds to $Q_{max} = 0.44 \text{ GW/m}^2$. (For interpretation of the references to color in this figure legend, the reader is referred to the web version of this article.)

the peaks and several times lower for toroidal positions between the injectors.

3.2. Wall heat load optimization

The Ne gas in each injector is stored in a plenum of 200 cm^3 volume with a pressure of up to 10 MPa. The maximum Ne gas amount in each injector is therefore $P_0 = 2 \text{ kPa m}^3$. This quantity can be reduced by reducing the pressure in the plenum.

The first wall temperatures during MGI of 2 kPa m^3 Ne from each of the three upper injectors and from the midplane injector are shown in Fig. 7. For this case, the melt threshold is reached at 4.6 ms. The melted surface area then grows and reaches of $S_{max} = 9.1 \text{ m}^2$ at 5.8 ms. The melt is fully re-solidified at 8 ms. The maximum wall temperature reached in this case is close to the vaporization temperature, $T_{max} = 2700 \text{ K}$ ($T_{vap} = 2744 \text{ K}$). The melting is mainly driven by the radiation heat load from the midplane injector because of the small distance between the separatrix and the wall at this location and the faster timescales. The melted area is indicated by a black line in the left panel of Fig. 7. The first wall does not melt in front of the upper injectors. It is interesting to compare these results to a case for which the injection takes place through the upper injectors only. The resulting temperature for an injection of 2 kPa m^3 Ne from each upper injector is shown in the right panel of Fig. 7. The maximum wall temperature in this case is $T_{max} = 1280 \text{ K}$, noticeably smaller than $T_{melt} = 1560 \text{ K}$.

A series of simulations with sequential twofold decrease of injected gas amount has been performed with the aim to reduce the first wall heat fluxes from the radiation flash and to identify the minimum quantity required to keep radiation levels high enough to ensure sufficient thermal quench mitigation in ITER. In accordance with our expectations, the reduction of the gas pressure in the plenum has led to reduction of the maximum radiated power and to stretching the heating pulse in time, as seen in Fig. 8. For the cases investigated, the peak wall temperature after irradiation of the entire plasma thermal energy is consequently reduced until 31 Pa m^3 of Ne is reached in the plenum. For this quantity the thermal energy is not fully radiated and approximately 18% of the initial thermal energy remains in the core. Simulation results for the case of 3 + 1 injector with 62 Pa m^3 of Ne, for which the plasma energy is still fully radiated, show a decrease of the maximum wall temperature below T_{melt} , to $T_{max} = 1490 \text{ K}$, whereas for a two times larger injection (125 Pa m^3) the wall still melts at 8 ms for $\sim 1.6 \text{ ms}$ with a melted area of $S_{max} = 1.4 \text{ m}^2$.

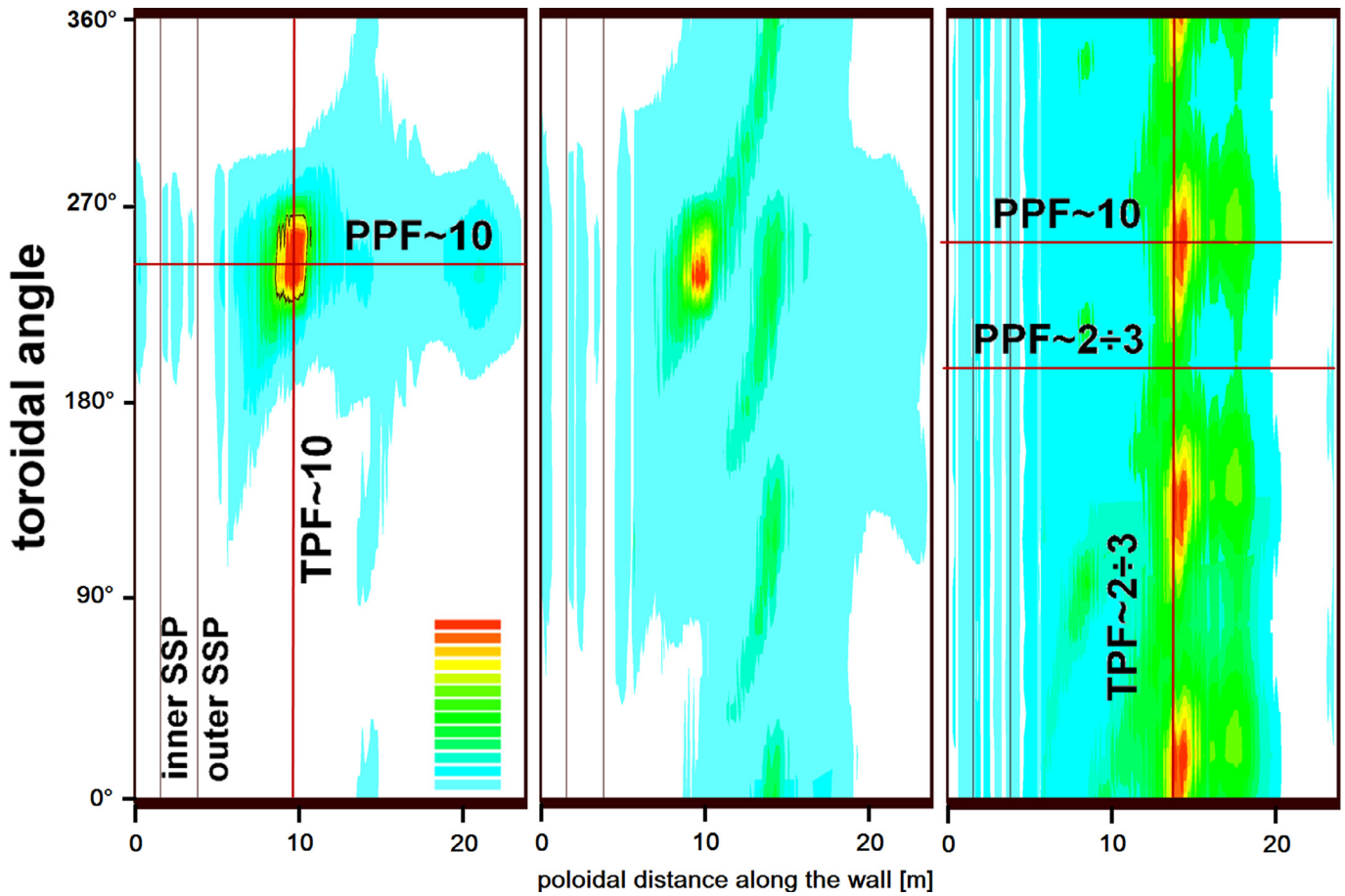


Fig. 7. The simulated wall temperature distribution for MGI of 2 kPa m^3 Ne from each of the three upper injectors and the midplane injector into an ITER plasma with thermal energy of 280 MJ is shown in the left and middle panels for two time moments: 6 ms, when most of the heat flux is caused by the midplane injector ($T_{max} = 2340 \text{ K}$) and 8 ms, when the heating of the wall is dominated by the upper injectors ($T_{max} = 1540 \text{ K}$). The right panel shows the wall temperature pattern for the case without midplane injector, $T_{max} = 1280 \text{ K}$. The black line in the left panel outlines the melted area. Positions and estimations for poloidal (PPF) and toroidal (TPF) peaking factors for the heat flux on the first wall are shown.

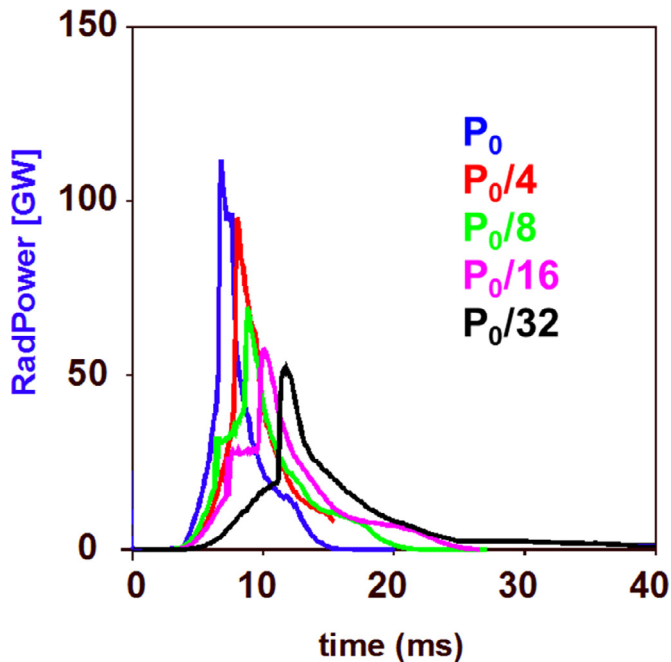


Fig. 8. Simulated total radiated power for different gas amounts in each of the four injectors ($P_0 = 2 \text{ kPa m}^3$). Ne gas has been injected into ITER plasma with thermal energy of 280 MJ.

4. Conclusions

Disruption mitigation by MGI in ITER has been simulated using an upgraded version of the TOKES code to take into account 3D effects of the penetration of the injected noble gas into the plasma and of the radiation heat loads on the ITER first wall. The simulations include the ITER first wall geometry and the set-up of the injectors of ITER DMS. The latter consists of 3 + 1 injectors: 3 upper and one midplane, containing up to 2 kPa m^3 of Ne gas each. The simulations have been performed for an H-mode ITER plasma with 280 MJ of plasma thermal energy. The efficiency of heat load mitigation has been assessed in the simulations with respect to injection quantity, to the number of injectors and their location.

The simulations have shown that first wall melting caused by the radiation flash during the mitigated thermal quench can be avoided by either reducing the quantity of injected neon or by using the upper port injectors only. Injection from the upper ports with the maximum amount of Ne – 2 kPa m^3 from each of the three injectors resulted in a temperature rise up to $T_{max} = 1280 \text{ K}$, well below the melt limit. Adding the midplane injector resulted in a drastic increase in the peak wall temperature, almost up to the vaporization temperature. The wall has been melted in this case over an area of $S_{max} = 9.1 \text{ m}^2$ and re-solidified after slightly more than 2 ms.

Simulations with reduced injection quantities have revealed a steady decrease of the radiation induced wall temperature. For the injection with all injectors, melting was prevented by reducing the

injected Ne amounts to 62 Pa m^3 from each injector. The maximum wall temperature reached was $T_{max} = 1490 \text{ K}$. Further reduction to 31 Pa m^3 of Ne led to insufficient radiation and part of the thermal energy was remaining in the plasma for more than 40 ms.

Further investigations of the first wall heat load mitigation during MGI in ITER are still needed. One can propose further wall damage mitigation adjusting time delays between injectors. These investigations are planned and the results will be reported in next papers. It is also important to note that the simulations presented here take into account asymmetries in radiation caused by the injection geometry, but a possible impact of the MHD events driving the thermal quench on poloidal and toroidal radiation distribution have not been considered so far. The effect of large scale MHD on the radiation distribution has been found in [10] to be equally significant with the Ne plasma spot dynamics.

Acknowledgments

This work was supported by Fusion for Energy and by the ITER Organization and carried out within the framework of the contract F4E-OPE-584. The views and opinions expressed herein do not necessarily reflect those of IO and F4E. ITER is a Nuclear Facility INB-174.

References

- [1] M. Lehnen, et al., Nucl. Fusion 51 (2011) 123010.
- [2] I. Landman, et al., Fusion Eng. Des. 88 (2013) 1682–1685.
- [3] I.S. Landman, Tokamak Code TOKES Models and Implementation, Report of Forschungszentrum Karlsruhe, 2009 FZKA-7496.
- [4] I.S. Landman, S.E. Pestchanyi, Y. Igitkhanov, R. Pitts, Two-dimensional modeling of disruption mitigation by gas injection, Fus. Eng. Des. 86 (2011) 1616.
- [5] S. Pestchanyi, M. Lehnen, A. Huber, I. Landman, Verification of TOKES simulations against the MGI experiments in JET, Fusion Eng. Des. 87 (2012) 1195–1200.
- [6] S. Pestchanyi, M. Lehnen, A. Huber, S. Gerasimov, Yu. Igitkhanov, I. Landman, et al., Analysis of energy cross-transport during MGI: JET experiments and TOKES simulations, Fusion Eng. Des. 88 (2013) 1127–1131.
- [7] S. Pestchanyi, A. Boboc, A. Bazylev, I. Landman, Optimization of MGI in JET using the TOKES code and mitigation of RE damage for the first wall, Fusion Eng. Des. 89 (2014) 2159–2163.
- [8] V.A. Izzo, Impurity mixing and radiation asymmetry in massive gas injection simulations of DIII-D, Phys. Plasmas 20 (2013) 056107.
- [9] D. Shiraki, N. Commaux, L.R. Baylor, N.W. Eidietis, E.M. Hollmann, V.A. Izzo, Characterization of MHD activity and its influence on radiation asymmetries during massive gas injection in DIII-D, Nucl. Fusion 55 (7) (2015) 073029.
- [10] V.A. Izzo, et al., The role of MHD in 3D aspects of massive gas injection, Nucl. Fusion 55 (2015) 073032.
- [11] A. Fil, et al., Three-dimensional non-linear magnetohydrodynamic modeling of massive gas injection triggered disruptions in JET, Phys. Plasmas 22 (2015) 062509.
- [12] S.I. Braginskii, in: M.A. Leontovich (Ed.), Reviews of Plasma Physics, vol. 1, Consultants Bureau, New York, 1965, p. 205.